An 8500-year history of climate-fire-vegetation interactions in the eastern maritime black spruce-moss bioclimatic domain, Québec, Canada

Augustin Feussom Tcheumeleu, Laurent Millet, Damien Rius, Adam A Ali, Yves Bergeron, Pierre Grondin, Sylvie Gauthier, Olivier Blarquez

ÉCOSCIENCE
https://doi.org/10.1080/11956860.2023.2292354

Taylor & Francis
Taylor & Francis Group

An 8500-year history of climate-fire-vegetation interactions in the eastern maritime black spruce–moss bioclimatic domain, Québec, Canada

Augustin Feussom Tcheumeleu [a,b], Laurent Millet [b], Damien Rius [b], Adam A. Ali [c], Yves Bergeron [d,e], Pierre Grondin [f], Sylvie Gauthier [g] and Olivier Blarquez [a]

[a]Laboratoire de Paléoécologie, Département de Géographie, Université de Montréal, Montréal, Canada; [b]Chrono-environnement UMR6249, CNRS, Université Franche-Comté, Besançon cedex, France; [c]Institut des Sciences de l'Évolution, Montpellier UMR 5554, CNRS-IRD-Université Montpellier-EPHE, Montpellier, France; [d]Centre d'étude de la Forêt, Université du Québec à Montréal, Montréal, Canada; [e]Institut de recherche sur les forêts, Université du Québec en Abitibi-Témiscamingue, Rouyn-Noranda, Canada; [f]Ministère des Forêts, de la Faune et des Parcs, Québec, Canada; [g]Natural Resources Canada, Canadian Forest Service, Laurentian Forestry Centre, Québec, Canada

ABSTRACT

The eastern, maritime portion of the black spruce – moss bioclimatic domain in Québec (Canada) is characterized by large wildfires with low occurrence. However, it is still poorly understood how climate–fire interactions influenced long-term vegetation dynamics in the boreal forest of eastern Québec. The long-term historical climate–fire–vegetation interactions in this region were investigated using a multiproxy (chironomids, charcoal, and pollen) paleoecological analysis of an 8500-year sediment core. Chironomid-inferred August air temperatures suggest that the warm Holocene Thermal Maximum (HTM; between ca. 7000–4000 cal yr BP) shifted to the cooler Neoglacial period (4000 cal yr BP to present), consistent with other temperature reconstructions across Québec. The shift to spruce-moss forest dominance around 4800 cal yr BP occurred nearly a thousand years before the climatic shift to the Neoglacial period and rather coincided with a shift from frequent low-severity small fires to infrequent but large and severe fire events. Our results suggest that long-term changes in the summer temperature are probably not the main factor controlling fire and vegetation dynamics in eastern Québec. It seems that, throughout the postglacial period, summer temperatures never fell below a threshold that could have induced a significant vegetation response.

RÉSUMÉ

La partie orientale et maritime du domaine bioclimatique de la pessière à mousse au Québec (Canada), est caractérisée par des grands incendies à très faible occurrence. Cependant, l'effet des interactions climat-feu sur la dynamique à long terme de la végétation dans la forêt boréale de l'est du Québec est peu connu. A l'aide d'une analyse paléoécologique multiproxies (chironomes, charbon de bois, pollen) d'une carotte sédimentaire de 8500 ans, nous avons documenté les interactions à long terme entre le climat, le feu et la végétation à l'est du Québec. Les températures de l'air du mois d'août reconstituées par les chironomes suggèrent que la période chaude de l'Optimum climatique Holocène (7000-4000 ans avant aujourd'hui (AA)) a cédé place à la période froide du Néoglaciaire (4000 ans AA à l'actuel) en cohérence avec les reconstitutions climatiques réalisées ailleurs au Québec. L'établissement de la pessière à mousses il y a environ 4800 ans s'est produit près d'un millier d'années avant la transition vers le Néoglaciaire et a plutôt coïncidé avec le changement de petits incendies peu sévères fréquents, à de grands incendies sévères peu fréquents. D'après nos résultats, les changements de températures estivales ne semblent pas jouer un rôle prépondérant dans la dynamique de la végétation et des feux dans l'est du Québec. Il semble que, tout au long de la période postglaciaire, les températures estivales n'aient jamais diminué sous un seuil qui aurait induit une réponse significative de la végétation.

ARTICLE HISTORY
Received 25 February 2023
Accepted 3 December 2023

KEYWORDS
Chironomids; climate change; climate-fire-vegetation interactions; Eastern Canada; fire history; Holocene

MOTS CLÉS
Chironomes; changement climatique; interactions climat-incendie-végétation; Est du Canada; histoire des incendies; Holocène

Introduction

In eastern Canada, modern boreal vegetation composition is driven mostly by climatic conditions (Saucier et al. 2009; D'Orangeville et al. 2018; Couillard et al. 2019a) and fire regimes (Gauthier et al. 2001; Baltzer et al. 2021; Couillard et al. 2022). The eastern portion of the black spruce – moss bioclimatic domain (Saucier et al. 2009) is a unique ecosystem at the circumboreal scale (Saucier et al. 2015). This ecosystem is characterized by low fire occurrence and a fire cycle of more than 300 years (Bouchard et al. 2008; Portier et al. 2016; Couillard et al. 2022). As a result, the

CONTACT Augustin Feussom Tcheumeleu feussoma@yahoo.co.uk Laboratoire de Paléoécologie, Département de Géographie, Université de Montréal, Campus MIL 1375, Avenue Thérèse Lavoie-Roux, Montréal QCH2V 0B3, Canada
Supplemental data for this article can be accessed online at https://doi.org/10.1080/11956860.2023.2292354.

region's forests consist mainly of old-growth stands (De Grandpré et al. 2009).

A recent synthesis of the postglacial vegetation and climate history of eastern Québec and Labrador (Fréchette et al. 2021) suggests that the initial forests were slow to close due to the persistence of a cold climate until ca. 7500 cal yr BP (calibrated years before present). The current regional vegetation was established about 4000 years ago (Fréchette et al. 2021). However, little is known about the postglacial vegetation history of some parts of eastern Quebec as data are missing across the territory. For example, it is still unclear whether the vegetation composition remained unchanged throughout the postglacial period and across the territory.

Long-term paleoecological and paleoclimate records are important for investigating long-term fire–vegetation interactions since direct measurements of climate and environmental changes are missing for the pre-instrumental period. However, previous studies (Bouchard et al. 2008; Gauthier et al. 2010; Cyr et al. 2012; Portier et al. 2018) looking at the structural and compositional characteristics of old-growth forests over time covered only the last three centuries. In addition, Couillard et al. (2021) used mineral soil charcoal to study past vegetation and fire dynamics, but no link was made to Holocene climate change. Much remains to be learned regarding the drivers of vegetation dynamics during the preindustrial period in the eastern portion of the black spruce – moss bioclimatic domain.

Available paleoecological studies in the eastern portion of the black spruce – moss bioclimatic domain, provide fragmentary knowledge of vegetation, climate, and fire in the Baie-Comeau region (Magnan and Garneau 2014; Remy et al. 2017), Sept-Îles region (Mott 1976; King 1986), Havre-Saint-Pierre region (Payette et al. 2013; Magnan and Garneau 2014; Sauvé 2016), and Blanc-Sablon region (Lamb 1980; Engstrom and Hansen 1985). Portier et al (2016, 2018) and Couillard et al. (2022) documented regional fire regimes, while Fréchette et al. (2021) presented the postglacial vegetation and climate history in eastern Québec and southern Labrador. However, to date, no paleoecological study, using a multiproxy approach, has been done to understand the postglacial history of climate, fire, and vegetation in the eastern portion of the black spruce – moss bioclimatic domain.

The aim of this study was to examine the relationship between vegetation dynamics and temporal changes in climate and fire activity in eastern Québec, where the current fire regime is currently characterized by a low occurrence of large severe fires (Portier et al. 2018). The climate-fire-vegetation interactions were investigated using a multiproxy (chironomids, charcoal, pollen) paleoecological analysis of an 8500 years core.

Material and methods

Study site

Lake Mista (51.10279 N −63.44291 W, ~500 m.a.s.l.; Figure 1) is a small (ca. 0.27 ha surface area) and shallow lake (5 m maximum depth) with no major inlet. Most of the water drains to the lake from a small forested watershed (ca. 8 ha). It is located in the eastern Canadian boreal forest, within the eastern portion of the black spruce – moss bioclimatic domain (Saucier et al. 2009). According to Dalton et al. (2020), the deglaciation of the study area occurred at approximately 10,300 cal yr BP. The landscape is hilly, dominated by undifferentiated till between numerous rock outcrops. The climate is relatively cold and rainy, with a mean annual temperature of −1°C, a mean August temperature of 13.5°C and mean total annual precipitation of 976 mm (reference period: 1981–2010; Régnière et al. 2017). The current vegetation surrounding lake Mista is dominated by black spruce (*Picea mariana* (Mill.) B.S.P.) with balsam fir (*Abies balsamea* (L.) Mill.), white spruce (*Picea glauca* (Moench) Voss), tamarack (*Larix laricina* (Du Roi) K. Koch) and white birch (*Betula papyrifera* Marsh.) as companion tree species. Groundcover vegetation is mostly composed of feather mosses (*Pleurozium schreberi*) with occasional patches of *Sphagnum* spp. Fire is a major natural disturbance (Gauthier et al. 2001), but windthrow (Pham et al. 2004), spruce budworm (*Choristoneura fumiferana* Clemens) and hemlock looper (*Lambdina fiscellaria* Guenée) outbreaks (De Grandpré et al. 2009; Morin et al. 2009) are also important disturbances.

Coring and chronology

In May 2017, a sediment core (373 cm total length) was retrieved from the deepest part of lake Mista using a Kajak-Brinkhurst gravity corer for the top 20 cm, and a 5 cm diameter modified Livingstone-type square-rod corer for the subsequent 353 cm. Sampling of the top 20 cm at 0.5 cm resolution was performed in the field using an extruder device. The 353 cm long core was retrieved in 4 successive and partly overlapping sections of 1 meter each.

The chronology of Lake Mista is based on accelerated mass spectrometry (AMS) radiocarbon (^{14}C) dating of five samples (Table 1). The five radiocarbon dates were calibrated to calendar ages (cal yr BP) using the IntCal20 software (Reimer et al. 2020). In addition, to obtain an age-depth model for the top sediment core, short-lived radionuclides (^{210}Pb, ^{226}Ra, ^{137}Cs, and ^{241}Am) were measured in the top 20 cm surface sediment using a gamma spectrometer. Measurements were made in a very low

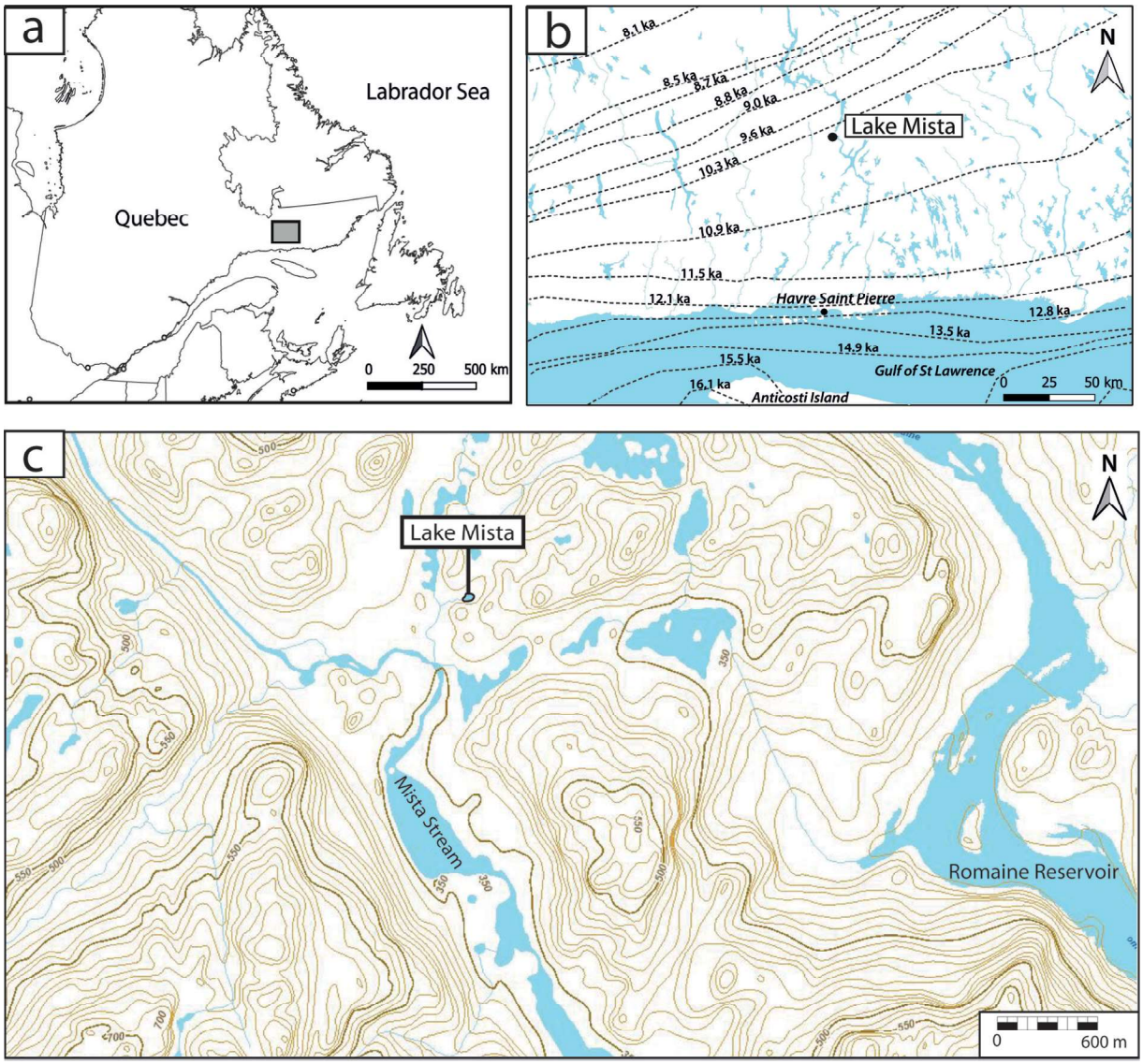

Figure 1. (a) location of the study area (grey square) in Québec-Labrador; (b) location of the study site (lake Mista) and deglaciation isochrones of the Laurentide ice sheet with ages in ka BP according to Dalton et al. (2020); and (c) location of the study site showing topography (https://vgo.portailcartographique.gouv.qc.ca/).

Table 1. ^{210}Pb and ^{14}C ages used for age-depth model of lake Mista sediment stratigraphy.

Laboratory code	Dated material	Depth (cm)	Radiocarbon age (^{14}C years BP, 1σ error)	Age cal BP (2σ error)
Pb-01	Sediment	0–1.5		–67
Pb-02	Sediment	1.5–2.5		–54 ± 1
Pb-03	Sediment	2.5–3.5		–48 ± 1
Pb-04	Sediment	3.5–4.5		–27 ± 4
Pb-05	Sediment	4.5–5.5		–12 ± 7
Pb-06	Sediment	5.5–6.5		8 ± 11
Pb-07	Sediment	6.5–7.5		11 ± 9
Pb-08	Sediment	7.5–8.5		16 ± 8
Pb-09	Sediment	8.5–9.5		33 ± 11
Pb-010	Sediment	9.5–10.5		71 ± 18
D-AMS 025608	Herbaceous stems	69–74	2103 ± 21	2064 (1997–2123)
D-AMS 025609	Herbaceous stems	151–156	3694 ± 27	4036 (3928–4145)
D-AMS 025610	Herbaceous stems	229–234	5109 ± 27	5812 (5751–5923)
D-AMS 025611	*Picea glauca* cone	342–343	7472 ± 33	8283 (8193–8367)
D-AMS 025612	*Picea glauca* cone	359–360	7741 ± 32	8511 (8430–8590)

background environment in the underground laboratory of Modane (LSM/Chrono-Environment Radionuclide Unit). Supported ^{210}Pb was determined from raw ^{226}Ra. The activity of excess ^{210}Pb in each sediment layer was determined from subtraction of total ^{210}Pb and supported ^{210}Pb (Supplemental Material S0). The equilibrium depth was reached at 10 cm based on the Constant Rate Supply (CRS; Appleby and Oldfield 1978) model. A composite age-depth model was built from the combination of ^{210}Pb and ^{14}C dates using the clam 2.2 (Blaauw 2010) and R 3.3.2 (R Core Team 2016) softwares.

Pollen analysis

Seventy-nine subsamples of 1 cm^3 each were taken at 4–5 cm intervals (i.e.100–120 years temporal resolution depending on sedimentation rate). Before extraction, a *Lycopodium* tablet was added to each subsample in order to calculate pollen concentration (grains cm^{-3}) and pollen accumulation rate (PAR; grains cm^{-2} year^{-1}). Pollen extraction followed standard methods described in Fægri and Iversen (1989).

Three hundred pollen grains were counted in each of the 79 subsamples. Counting was performed under a light microscope at 400× magnification. Pollen grains were identified for family, genus, and species levels following Richard (1970), McAndrews et al. (1973) and the reference collection of the University of Montréal paleoecology lab. Differentiation of *Picea mariana* and *Picea glauca* pollen grains was based on their morphological characteristics (i.e., saccus shape, position of attachment of saccus to corpus, density and arrangement of internal reticulate structure of saccus, corpus area differences; Richard 1970; Hansen and Engstrom 1985). The *Betula* pollen grains were identified at genus level as we did not differentiate birch tree species (e.g., *Betula alleghaniensis* Britton, *Betula papyrifera* Marshall) and shrubby birch species (e.g., *Betula glandulosa* Michaux) by measuring their pollen diameter size (Richard 1970).

Charcoal analysis and fire regime reconstruction

Macroscopic charcoal extraction and counting

Contiguous subsamples of 1 cm^3 taken at 1 cm intervals were soaked in aqueous 8% sodium hypochlorite (NaClO) during 24 h in order to bleach non-charcoal organic matter. The subsamples were wet, sieved through a 150 µm mesh, then transferred to a Petri dish for counting (charcoal abundance) and measuring (charcoal area) macroscopic charcoal particles under a stereomicroscope coupled with the WINSEEDLE 2016 software (Regent Instruments Canada Inc.). The macroscopic charcoal particles (≥150 µm) were expected to come from a mix of local and regional fire events having occurred less than 10 km from the lakeshore (Oris et al. 2014; Hennebelle et al. 2020).

Reconstruction of paleofire history

Statistical analyses of charcoal data were performed using the CharAnalysis 1.1 program (Higuera et al. 2009). The sedimentation rate (cm^2.year^{-1}) obtained from the age-depth model, was used to calculate charcoal accumulation rates (CHAR; mm^2 cm^{-2} year^{-1}), from the measured area (mm^2) of charcoal pieces (Whitlock and Anderson 2003). The CHAR series were interpolated to a median sample resolution of 23 years in order to remove bias induced by variable sedimentation rates (Higuera et al. 2010), then separated into local fires (CHAR peak) and nonlocal or redeposited charcoal (CHAR background). CHAR background was estimated using a 500-year moving window with LOWESS smoother robust to outliers (Higuera et al. 2008). This window width captured centennial-scale variation in CHAR series. It was least affected by the high-frequency CHAR peaks (Gavin et al. 2006) and provided the best signal-to-noise index (SNI >3; Kelly et al. 2011; Brossier et al. 2014). The locally defined CHAR peak was calculated by subtracting the CHAR background from the interpolated CHAR series. The CHAR peak component was split into two subcomponents (CHAR peak noise (non-fire event) and CHAR peak signal (fire event) using a Gaussian mixture model (Higuera et al. 2007). A 99th percentile cutoff of the noise distribution was considered as the threshold value for fire event identification. Fire occurrence (number of fire events per 1000 years) was estimated by smoothing the CHAR peak signal, with a 1000-yr moving window. The cutoff probability for the minimum count analysis value was set to 1. The fire return intervals (FRIs) were calculated from the CHAR series. CHAR peak magnitude was used as an indicator of fire size and/or severity (Higuera et al. 2005; Ali et al. 2012).

Chironomid analysis and temperature reconstruction

Paleotemperatures were reconstructed from chironomids, a climate proxy independent of pollen. Chironomids are a useful paleoecological proxy because of their abundance and taxonomic diversity, their possible identification to subfamily, tribe, genus, or even species group levels, the good preservation of their head capsules in lake sediments, their sensitivity,

and their rapid response to environmental changes (Walker 1987). Direct and indirect relationships between air temperature, water temperature, and distribution of chironomid communities enable the development of chironomid-based transfer functions and quantitative temperature reconstructions (Eggermont and Heiri 2012).

Chironomid extraction, identification, and counting

Seventy-nine subsamples of wet sediments were taken at 4–5 cm intervals, at the same depths as for pollen analysis. The size of each analyzed subsample was adjusted to have a minimum count of 50 head capsules. Chironomid head capsule extraction and mounting followed standard preparation technique described in Brooks et al. (2007). Specimen identification was performed under a light microscope at 400× magnification. The identification of chironomid specimens to genus and species-group relied on several keys (e.g., Larocque and Rolland 2006; Brooks et al. 2007; Andersen et al. 2013; Larocque-Tobler 2014).

Temperature reconstruction

For Canada, several transfer functions are now available to infer summer air temperatures from subfossil assemblages of Chironomidae (i.e., Larocque 2008; Fortin et al. 2015; Medeiros et al. 2022). These inference models are built on the study of the modern distribution of subfossil Chironomidae assemblages in lake surface sediments distributed along latitudinal climate gradients. They differ in the number of modern sites, their geographical distribution, the climatic gradient covered, and the taxonomic resolution of chironomid taxa identification (Supplemental Material S1a, b). For this study, we chose to use the transfer function of Larocque (2008). Indeed, based on their performance statistics (Supplemental Material S1a), the transfer function (TF) of Larocque (2008) was more likely to yield accurate reconstructions. The temperature reconstruction patterns obtained with other TFs were similar (Supplemental Material S1c), but the ones obtained using the Larocque (2008) TF yielded values closer to the monitored values for the current period (13.5°C; Régnière et al. 2017).

The eastern Canadian modern calibration dataset of Larocque (2008) comprises 75 lakes and 79 taxa. This calibration dataset covered August air temperature ranging from 3°C to 21°C i.e., an 18°C gradient. Two components Weighted Averaging Partial Least-Squares regression (WAPLS) served as inference model and bootstrapping was used to estimate the sample-specific errors for the fossil samples. Taxa absent from the modern calibration dataset were removed from the fossil dataset (Birks et al. 1990). The robustness of the inferred August air temperature was assessed by calculating (1) the chi-square distance to the closest modern assemblage; (2) the goodness-of-fit with temperature (Birks et al. 1990); (3) the percentage of chironomid taxa considered to be rare in the modern calibration dataset (i.e., with a Hill's N2 (Hill 1973) less than 5; Heiri et al. (2003); (4) the statistical significance of the reconstructions (Telford and Birks 2011). Based on their chi-square distance to the closest modern assemblage, fossil chironomid assemblages were identified to be 'good analogs' (if the chi-square distance was within the 1^{st}-5^{th} percentiles), 'poor analogs' (>10^{th} percentile and < 20^{th} percentile) or 'no analog' (>20th percentile). Goodness-of-fit to temperature was assessed by passively fitting fossil samples to the canonical correspondence analysis (CCA) of the modern calibration dataset with August temperature as the only constraining parameter. Fossil samples with a squared residual length to CCA axis 1 above the 90^{th} and 95^{th} percentiles of the residual distances of all modern samples were considered as having a 'poor fit' and 'very poor fit' with temperature respectively (Birks et al. 1990). The percentage of chironomid taxa considered to be rare in the modern calibration dataset was estimated with the 'compare' function in analogue R package (Simpson 2007). The chironomid effective diversity (Hill's N2 index) was measured using the utility function in rioja R package (Juggins 2014).

Numerical and statistical analysis

Both the pollen percentage diagram as well as the chironomid abundance diagram were plotted using the strat.plot function in the rioja R package (Juggins 2014). Zonation of the pollen and chironomid percentage diagrams were defined using stratigraphically constrained cluster analysis (CONISS; Grimm 1987). For both proxies, the number of statistically significant assemblage zones was determined by applying the broken-stick model (Bennett 1996).

A detrended correspondence analysis (DCA) was performed separately on the chironomid and pollen percentage matrix using the decorana command in the vegan R package (Oksanen et al. 2018). Only chironomid taxa and pollen taxa present in at least two samples and with a relative abundance higher than 2% in at least one sample were included in the analysis. The length of each first axis of the DCA determined whether the distribution pattern of each proxy along the DCA axis 1 was linear or unimodal (Borcard et al. 2011). Following the gradient length of the DCA axis 1 (chironomid: 1.44 standard deviation (SD) units; pollen: 1.15 SD), a principal component analysis (PCA) was performed

on the pollen and chironomids square-root-transformed percentage matrix in order to highlight main changes in assemblage composition during the postglacial period.

Results

Chronology

Radiocarbon (^{14}C) and ^{210}Pb dating were used to generate the age-depth model showing a mean sedimentation rate of ~0.045 cm per year. The extrapolation of the age-depth model to the bottom of the core (373 cm) suggests that the accumulation of organic sediment began at ca. 8500 cal yr BP (Figure 2). The top 10 cm represents ca 150 years (from 1880 to 2017 AD).

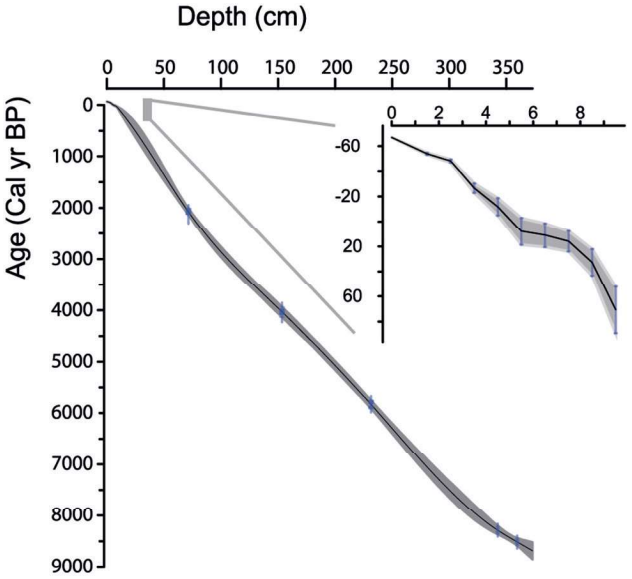

Figure 2. Age-depth model of lake Mista based on ^{14}C and ^{210}Pb dates. The black line represents the inferred chronology modeled using a smoothing spline function (spar = 0.3). The 95% confidence intervals for the model are shown in grey.

Pollen record

The stratigraphically constrained cluster analysis of the Lake Mista pollen record indicated eight significant pollen assemblage zones (PAZ-1 to PAZ-8; Figure 3).

PAZ-1 (ca. 8500–8100 cal yr BP)

PAZ-1 corresponds to progressive afforestation of the vicinity of the lake, with high values of *Picea mariana* (37–73%), *Betula* spp. (9–22%) and *Alnus crispa* (Aiton) Raus (6–15%). Cones of *Picea glauca* found at 359.5 and 342.5 cm (Table 1) confirm that more than 8500 years ago, the vegetation surrounding Lake Mista already hosted *Picea glauca* populations mature enough to reproduce.

PAZ-2 (ca. 8100–7800 cal yr BP)

Abies balsamea (25–46%) settled in the vicinity of the lake during PAZ-2. They dominated with *Betula* spp. (22–32%), perhaps with *Alnus crispa* (5–12%). *Picea glauca* (5–9%) was probably still present and *Picea mariana* (8–13%) decreased in abundance (Figure 3; Supplemental Material S2).

PAZ-3 (ca. 7800–6700 cal yr BP)

Abies balsamea (7–19%) remained present, although less abundant during PAZ-3. Despite the rising percentage of

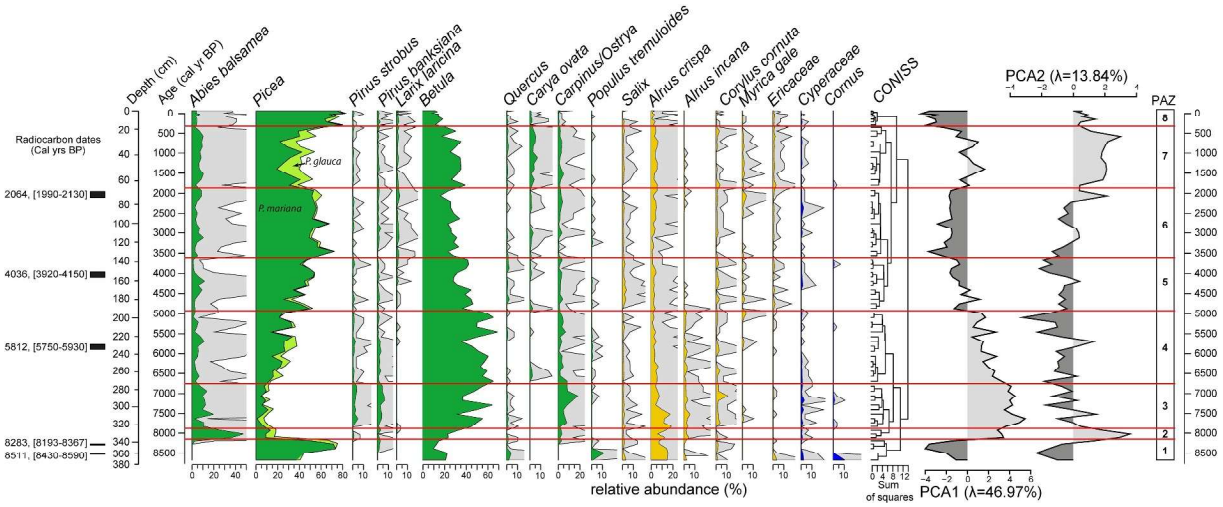

Figure 3. Simplified pollen percentage diagram, with trees (green), shrubs (yellow), and herbs (blue). The CONISS cluster dendrogram is also shown. Pollen PC axis 1 and axis 2 sample scores (λ indicates the proportion of variance explained by the PC axis of the fossil data), and pollen assemblage zones (PAZ; horizontal solid red lines) are also displayed.

Betula spp. (30–63%), the influxes (Supplemental Material S2) show that their populations have not increased around the lake. *Carpinus/Ostrya* grains likely represent increased pollen inputs from the south, perhaps due to an opening of the regional forest, also indicated by low values of total pollen influx (Supplemental Material S2). The boundary between PAZ-3 and PAZ-4 marks the end of afforestation.

PAZ-4 (ca. 6700–4800 cal yr BP)

PAZ-4 is a transitional zone marked by a regional increase in *Picea mariana* tree populations as supported by the pollen percentages (12–33%; Figure 3) and influxes (Supplemental Material S2). *Betula* spp. (34–68%) reached its maximum postglacial abundance according to pollen percentages and influxes (Figure 3; Supplemental Material S2). *Picea glauca* (1–12%) was probably still present according to the influxes. From PAZ-4 to PAZ-8, the pollen influx trends of major taxa (Supplemental Material S2) show the same pattern as their pollen percentages (Figure 3).

PAZ-5 (ca. 4800–3600 cal yr BP)

Picea mariana tree populations continued to increase in PAZ-5. Subsequently, *Picea mariana* (25–54%) became the dominant taxon with *Betula* spp. (27–45%) and *Abies balsamea* (1–11%) as companion tree species.

PAZ-6 (ca. 3600–1800 cal yr BP)

Picea mariana (49–72%) dominated the forest canopy in PAZ-6. *Abies balsamea* (2–10%) was still a companion species, whereas *Betula* spp. (15–33%) slightly decreased. *Picea glauca* (1–9%) was scarcer than before and thereafter. *Alnus crispa* (1–5%) experienced a modest revival, without abounding.

PAZ-7 (ca. 1800–300 cal yr BP)

Picea mariana (19–57%) regressed in PAZ-7 and was likely replaced by *Picea glauca* (5–20%) (see percentage and influx; Figure 3 and Supplemental Material S2). *Carya ovata* (Miller) K. Koch. (1–6%) showed surprisingly high percentages and its influxes increased (Figure 3; Supplemental Material S2).

PAZ-8 (ca. 300 cal yr BP to present)

PAZ-8 marks the closure of the forest cover. *Picea mariana* (63–81%) increased (see influx; Supplemental Material S2). *Betula* spp. (7–18%) regressed but *Abies balsamea* (3–7%) remained a companion tree in the spruce moss forest.

Charcoal record

During the past 8500 years, there were 49 fire events with a mean FRI of 181 years (95% confidence interval 149–215 years) and a range of 111 to 331 years (Figure 4). The signal-to-noise index at 163 cal yr BP (SNI = 2.85) and from ca. 140 cal BP to present (SNI = 0) were unreliable due to difficulties in separating CHAR peak noise (non-fire event) and CHAR peak signal (fire event). Excluding these periods, the SNI values were above 3, with a median value of 8.49 for the entire sequence, supporting therefore their reliability for the reconstruction of local fire activity (Courtney-Mustaphi et al. 2015).

Four periods with distinct fire occurrence can be distinguished in the record (Figure 4). From 8500 to 5000 cal yr BP, fire occurrence dropped from its highest level of 9, to 4 fires kyr^{-1}. Between 5000 and 3600 cal yr BP, fire occurrence reached its lowest values and varied between 2 and 4 fires kyr^{-1}. Peak magnitudes were larger than before 5000 cal yr BP. From 3600 to 1300 cal yr BP, fire occurrence increased slightly from 4 to 6 fires kyr^{-1}. The largest peak magnitude was recorded during this period. After 1300 cal yr BP, fire occurrence dropped to present day 3 fires kyr^{-1}. A notable peak magnitude was recorded around 1000 cal yr BP. The lowest and highest FRI values were reached at ca. 8500 cal yr BP (111 yr/fire) and ca. 4000 cal yr BP (331 yr/fire), respectively.

Chironomid stratigraphy and inferred August temperature

The chironomid record was split into two significant chironomid assemblage zones (CAZ-1 and CAZ-2; Figure 5) due mainly to changes in *Micropsectra insignilobus*-type relative abundance. This biozonation suggested by the stratigraphically constrained cluster analysis is further supported by the sharp increase in chironomid PC axis 1 sample scores (Supplemental Material S3a).

CAZ-1 (ca. 8500–1200 cal yr BP)

Micropsectra insignilobus-type abundance was less than 15% throughout CAZ-1, which was further divided into three sub-biozones (CAZ-1a to CAZ-1c) according to minor changes in some chironomid taxa.

CAZ-1a (ca. 8500–8100 cal yr BP) was characterized by the dominance of cold stenotherm taxa such as *Heterotrissocladius marcidus*-type, *Chironomus anthracinus*-type, *Corynocera oliveri*-type, *Tanytarsus lugens*-type, and *Sergentia coracina*-type (Brooks et al. 2007). A notable and characteristic presence (at less than 2%) of chironomids with colder optima (e.g., *Heterotrissocladius*

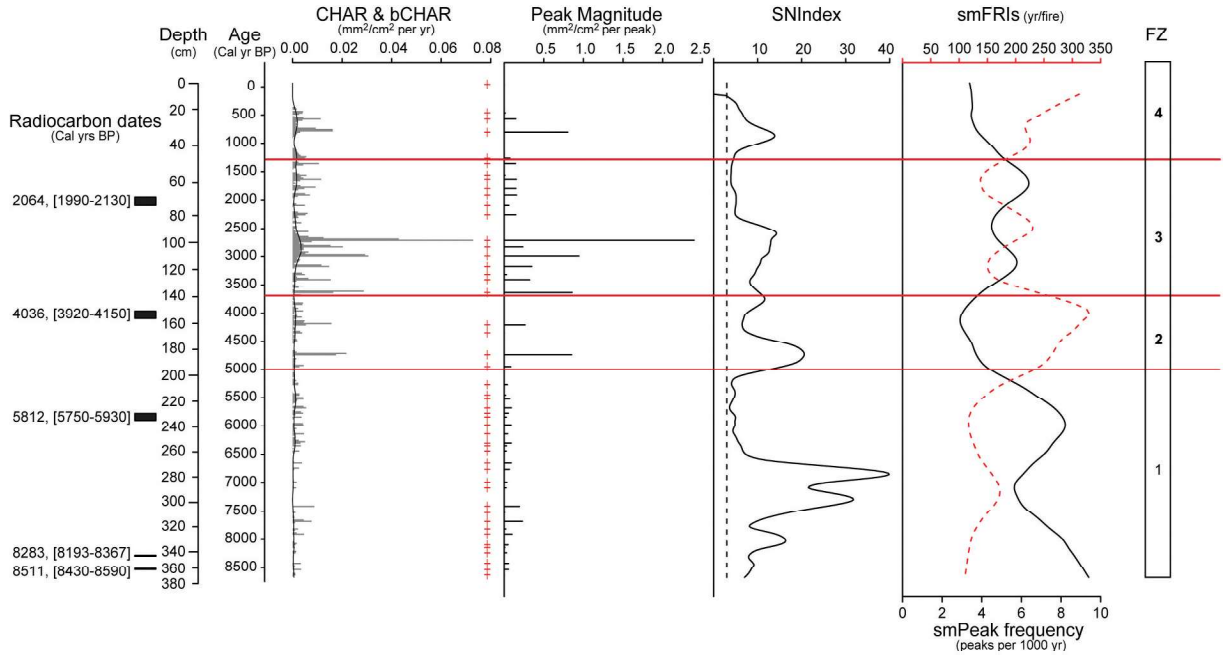

Figure 4. Charcoal accumulation rates (CHAR), CHAR background (bCHAR), fire events, peak magnitude of fire events, signal-to-noise index (threshold value of 3: vertical dashed black line), fire occurrence (smPeak frequency) and return interval (smFris). Fire zones (FZ; horizontal solid red lines) are also shown.

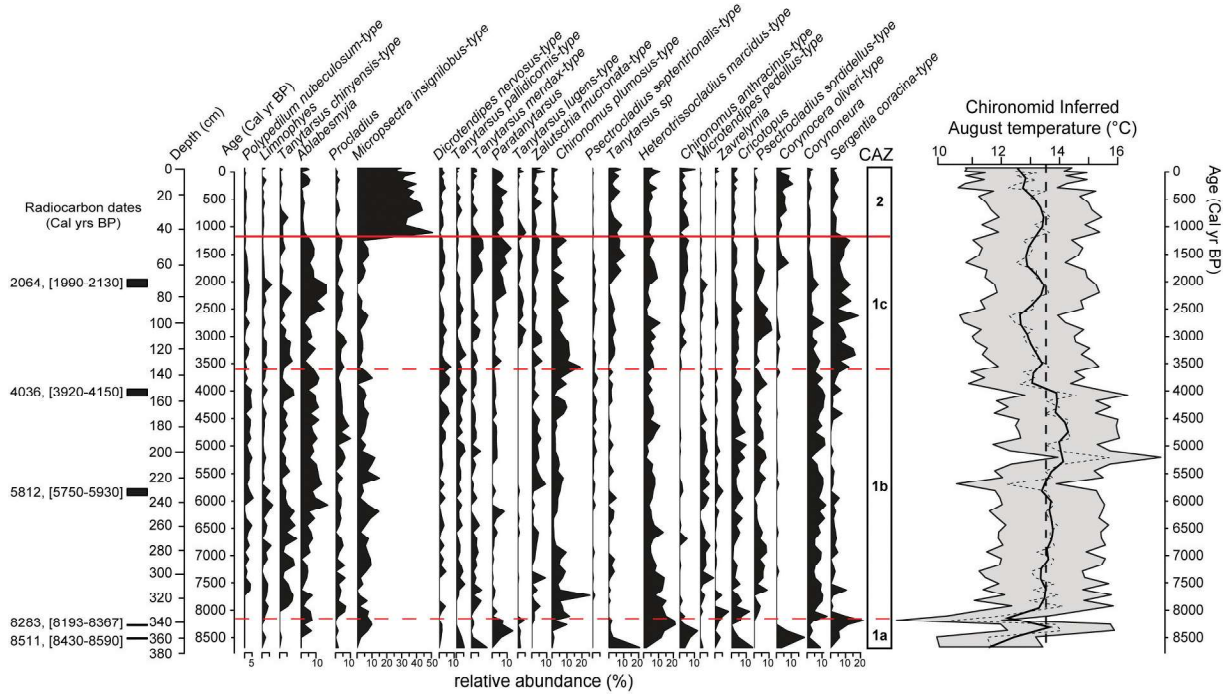

Figure 5. Simplified chironomid percentage diagram, chironomid assemblage zone (CAZ; in horizontal solid red line, sub-biozones in horizontal dashed red lines), chironomid inferred August temperature (dashed black line; with a LOWESS smoother in solid black line (span = 0.073), with the grey area delimiting the minimum and maximum sample-specific estimated standard error of prediction (eSEP)). Present day August temperature (13.5°C; Régnière et al. (2017)) is also shown (vertical dashed black line).

subpilosus-type, *Paracladopelma*, *Pseudodiamesa*, *Protanypus*, *Diplocladius*; Supplemental Material S3b; Brooks et al. 2007) suggests that a particularly cold phase occurred over a short period centered on 8200 cal yr BP.

CAZ-1b (ca. 8100–3600 cal yr BP) was characterized by the high abundance of *Ablabesmyia*, *Heterotrissocladius marcidus*-type, *Micropsectra insignilobus*-type, *Corynoneura*, and *Tanytarsus chinyensis*-type. There was a notable development of taxa associated to aquatic macrophytes like *Limnophyes*, *Polypedilum nubeculosum*-type, *Chironomus plumosus*-type, *Psectrocladius sordidellus*-type, and *Microtendipes pedellus*-type (Brooks et al. 2007; Millet et al. 2007, 2012). The abundance of *Polypedilum nubeculosum*-type between ca. 7500–4000 cal yr BP, a taxon with warm optima in European and Canadian modern data sets (e.g., Larocque 2008; Heiri et al. 2011), suggests warm conditions.

CAZ-1c (ca. 3600–1200 cal yr BP) was characterized by an increase in *Sergentia coracina*-type. From ca. 3600 cal yr BP, there was a decrease in *Polypedilum nubeculosum*-type, a taxon characteristic of warm eutrophic lakes, in favor of taxa indicative of cold and well-oxygenated oligotrophic lakes such as *Sergentia coracina*-type, *Chironomus anthracinus*-type, *Tanytarsus lugens*-type, *Heterotrissocladius marcidus*-type, and *Corynocera oliveri*-type (Brooks et al. 2007).

CAZ-2 (ca. 1200 cal yr BP to present)

CAZ-2 was characterized by the dominance of *Micropsectra insignilobus*-type, a cold stenotherm chironomid characteristic of well-oxygenated oligotrophic lake environments (Brooks et al. 2007). The presence of *Corynocera oliveri*-type and *Sergentia coracina*-type likely supports the assumption of cold conditions (Brooks et al. 2007). On the other hand, around ca. 1200 cal yr BP the drop in the relative abundance of cold indicating taxa (e.g., *Sergentia coracina*-type) before rising again at ca. 500 cal yr BP probably marked a warmer phase between 1200 and 500 cal yr BP. The reappearance of *Heterotrissocladius subpilosus*-type, *Protanypus,* and *Diplocladius* at ca. 300 cal yr BP (Supplemental Material S3b) implies a very cold and ultraoligotrophic lake environment at the time (Brooks et al. 2007).

Out of the 79 fossil samples, 51 samples had 'poor' analogs, while 12 others had 'no' analog with the calibration dataset. The bottom sample had a very poor fit to temperature, while eight other samples within the sequence had a poor fit with temperature (Supplemental Material S3c). All fossil samples contained less than 20% (range 4.3–17.48%) of rare taxa in the training set (Supplemental Material S3c) as needed to obtain reliable estimation of temperature from a fossil sample (Brooks and Birks 2001; Larocque-Tobler 2010). The sample-specific estimated standard error of prediction (eSEP) for inferred temperature varied between 1.67 and 1.92°C. Inferred temperatures were statistically significant ($p = 0.041$) when compared to 999 random reconstructions as recommended by Telford and Birks (2011).

Chironomid inferred August temperature (Figure 5) suggests a warming climate from ca. 8500 to 4000 cal yr BP (average temperature 13.5°C; range 10.2–15.7°C) followed by a cooling trend from ca. 4000 cal yr BP to present (average temperature 13°C; range 12.2–13.7°C).

Discussion

Temperature reconstruction

Reliability of the chironomid-inferred mean August air temperature

The chironomid stratigraphy suggests that other environmental and limnological factors than summer temperature may have played a role on assemblage changes. These factors may ultimately be related to the climate, but because of the indirect nature of the relationship between chironomid assemblages and climate, it is necessary in this case to go further in assessing the reliability of the chironomid inferred August temperature by looking at the diagnostic elements (i.e., rare taxa, fit to temperature, modern analogs).

Rare taxa. All fossil samples had at least 82% of their taxa represented in the modern training set (i.e., beyond the 80% objective criterion; Larocque-Tobler 2010). Inferred temperatures are likely to be less well estimated for 38 fossil samples containing more than 10% of taxa that are considered to be rare taxa in the training set (Brooks and Birks 2001). This concerned particularly the period before 4000 cal yr BP (Supplemental Material S3c) in which all fossil samples had poor or no analog. However, the WAPLS regression performs well even under non-analog situations once the above-mentioned rare taxa objective criterion is met (Birks and Birks 1998).

Fit to temperature. After 6000 cal yr BP, all fossil assemblages were well fitted by temperature. The eight fossil assemblages which are poorly or very poorly fitted by temperature before 6000 cal yr BP suggest that other controlling factors than climate may have punctually influenced chironomid changes between ca. 8500 and 6000 cal yr BP (Velle et al. 2005, 2010). Therefore, the inferred temperatures for this period should be interpreted with caution. Indeed, in-lake variables can

influence chironomid assemblages over shorter timescales (Brodersen and Quinlan 2006). Multiple factors likely controlled chironomid distributions. Nevertheless, the period before 6000 cal yr BP was documented by a total of 24 samples, with two-thirds (i.e.16) having their assemblages well fitted by temperature.

Modern analog. Although the present-day temperature was within the error margin of our reconstructions, the accuracy of the chironomid inferences, especially for the period before 4000 cal yr BP that had the highest number of rare taxa and also poor or no analog, could be improved by sampling and adding more lakes with temperatures between 16 and 19°C to the calibration set as earlier suggested by Bajolle et al. (2018). The majority of fossil samples having a high number of rare taxa and also poor or no analog were found during the warmest period suggesting that the lake environment was probably different from the current situation. Therefore, the best analogs for early and mid-Holocene assemblages are likely to be found in present-day southern lakes. The reconstructed modern temperature differed from present day mean August temperature of 13.5°C likely because surface sample had poor analogs in the training set or because the top surface sample was missing.

Thus, interpretations of August-temperatures reconstructed from Chironomidae assemblages will be restricted to major changes that have occurred at millennial to multi-millennial time scales.

Chironomid-inferred major climatic periods

Holocene thermal maximum (HTM): ca. 7000–4000 cal yr BP. The chironomid inferred reconstructions (Figures 5, 6) suggest that warm temperatures were recorded in the Lake Mista region between ca. 7000 and 4000 cal yr BP. This corresponds to the HTM, which mostly occurred between 7000 and 5000 in northeastern North America (Renssen et al. 2012). For instance, in eastern Québec and Labrador (Eastern Canada), pollen-based reconstructions indicated maximum temperatures between ca. 7500 and 3500 cal yr BP (Fréchette et al. 2021). The timing and duration of the HTM depends on various forcings including orbitally forced insolation, the deglaciation of the Laurentide Ice Sheet (LIS) and the atmospheric greenhouse gases (Renssen et al. 2012). For Québec, the presence of the LIS and its decay may partly explain the differences observed between the sites depending on their proximity to LIS remnants (Fréchette et al. 2021).

In western Québec, chironomid inferred August temperatures were warmer with high magnitude values during the HTM (Bajolle et al. 2018). The low magnitude values at lake Mista may partly be due to the increasing east-to-west temperature gradient of continentality in the black spruce-moss bioclimatic domain (Saucier et al. 2009; Couillard et al. 2019a).

Neoglacial period: ca. 4000 cal yr BP to present. The chironomid-based temperature reconstructions from Mista suggest that after 4000 cal yr BP, temperature decreased and were about 1°C cooler than those recorded before this turning point (Figure 6). This cooler period corresponds to the so-called Neoglacial period. Indeed, at mid and high latitudes of the Northern Hemisphere, climate gradually shifted from a warm HTM to a cool Neoglacial with steadily decreasing summer insolation (Ali et al. 2012). Compared to other inferred temperature records across Canada (Gajewski 2015; Bajolle et al. 2018; Fréchette et al. 2018, 2021), the onset of the Neoglacial period was delayed in some areas of Quebec and Labrador until after 3200 cal yr BP (Gajewski 2015). Close to our study site, in Havre Saint Pierre, the peat-based paleohydrological records indicated that the Neoglacial cooling characterized by major changes in peat accumulation rate and bog surface moisture began around 3000 cal yr BP (Magnan and Garneau 2014).

The Neoglacial period was probably characterized by a series of higher frequency climate variability that should be interpreted cautiously because the variations remain within the error margin of the inferred temperatures (Supplemental Material S3c).

Climate-fire-vegetation interactions

The vegetation history was marked by two major phases (Figure 6), afforestation (8500–6700 cal yr BP) and forest phases (6700 cal yr BP to present).

Afforestation phase 8500–6700 cal yr BP

Spruce-moss forest 8500–8100 cal yr BP. Pollen assemblages from the bottom of the core suggest that vegetation – a *Picea mariana*-dominated woodland or forest – gradually colonized the ice-free areas following the slow decay of the Laurentide Ice Sheet (Blarquez and Aleman 2015; Richard et al. 2020; Fréchette et al. 2021).

Balsam fir-birch forest 8100–6700 cal yr BP. Starting from 8100 cal yr BP, the prevailing warm temperatures were suitable (Sims et al. 1990; Bergeron et al. 2014) to the establishment of *Abies balsamea-Betula* spp. mixed-woods. Smaller and less severe fires likely due to wet conditions between 7350 and 6560 cal yr BP (Magnan and Garneau 2014) probably exempted some areas from burning, allowing *Abies balsamea*

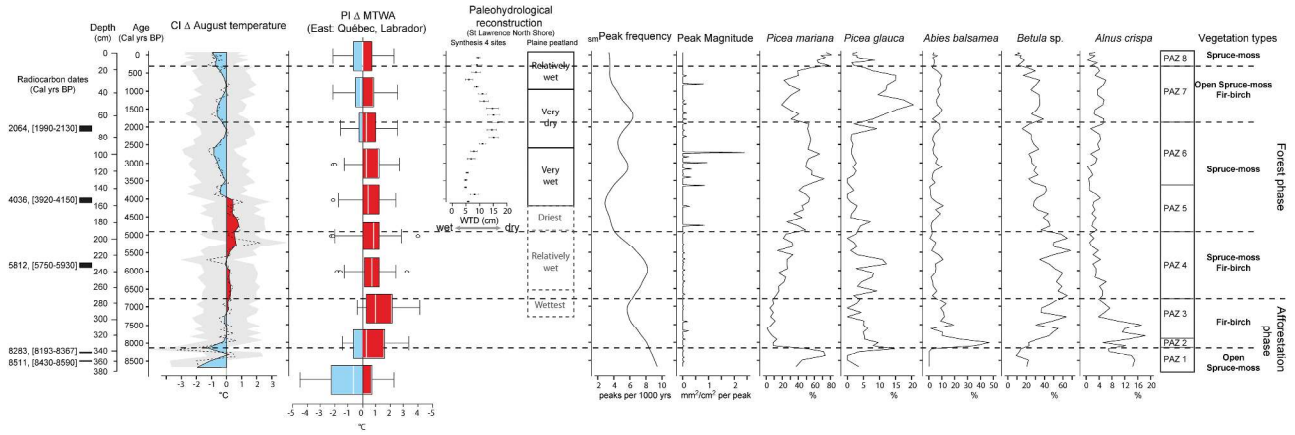

Figure 6. Climate-fire-vegetation interactions. From left to right: chironomid inferred August temperature anomaly, mean temperature of the warmest month (MTWA; eastern Quebec and Labrador) presented by box-plot every 1000 years and expressed as an anomaly relative to the current period ((Δ) (Fréchette et al. 2021),; synthesis of the reconstructed water table depths from four peat records since 4200 cal yr BP (mean water table depth (WTD) with standard errors calculated for each 200-year period (Magnan and Garneau 2014).; Summary of water table depth changes from the records of Plaine peatland (Havre St-Pierre) for the last 7000 cal yr BP (Magnan and Garneau 2014), fire occurrence (smPeak frequency), peak magnitude of fire events, pollen abundance of main taxa (*Picea mariana*, *Betula* spp., *Picea glauca*, *Abies balsamea*, *Alnus crispa*), pollen assemblage zone (PAZ; in horizontal solid grey lines) and vegetation types (in horizontal dashed grey lines) from lake Mista.

and *Betula* spp (mostly *Betula papyrifera*; Fréchette et al. 2021). from remnant stands to reinvade burned areas (Asselin et al. 2001; Bergeron et al. 2004). The very low abundance of *Picea mariana* pollen could question the actual presence of the species in the local vegetation at that time (Payette 1993). However, based on macro-remains, Couillard et al. (2018) confirmed the local presence of *Picea mariana* and *Abies balsamea* not later than 8300 cal yr BP south of Lake Mista. Furthermore, Couillard et al. (2019b) dated a spruce charcoal aged 8725 cal yr BP. Therefore, the observed decline of *Picea mariana* at the expense of *Abies balsamea* could be the result of a primary succession where *Picea mariana* is being overtaken by the late successional species (*Abies balsamea*) under longer fire cycle (Couillard et al. 2021). Then it was not until ca. 4800 cal yr BP that *Picea mariana* returned, perhaps favored by severe or larger fires (Figure 6).

Abies balsamea dominated boreal forests were also observed in the Sept-Îles region between 8000–6500 cal yr BP (Mott 1976; King 1986) and in southeastern Labrador (Lamb 1980; Engstrom and Hansen 1985). Maximum abundance of *Abies balsamea* from ca. 8100 to 6700 cal yr BP (Figure 6) is also consistent with Fréchette et al. (2021).

Forest phase 6700 cal yr BP to present

Spruce-moss balsam fir-birch forest 6700–4800 cal yr BP. Warmer climatic conditions coupled with smaller and less severe fires (Figure 6) due partly to wet climatic conditions between 6560 and 4800 cal yr BP (Magnan and Garneau 2014), created a propitious environment for the recruitment and proliferation of *Betula papyrifera*, *Picea glauca* and *Abies balsamea*. The wet climatic conditions may also have supported the decreasing trend in fire occurrence. Such species assemblage (*Picea mariana*, *Betula papyrifera*, *Picea glauca* and *Abies balsamea*) is observed in modern boreal mixed-wood (Sims et al. 1990; Galipeau et al. 1997). According to Fréchette et al. (2021), the pollen percentage values of *Betula* spp., *Picea mariana* and *Abies balsamea* (Figure 6) suggest the presence of two postfire successional pathways as described by Couillard et al. (2021) at the stand scale. The first pathway, from *Betula* spp. to *Abies balsamea* with presence of *Picea glauca* (*Abies balsamea-Picea glauca-Betula* spp.), and the second pathway from *Picea mariana* to *Abies balsamea*.

Spruce-moss forest 4800–1800 cal yr BP. 4800 cal yr BP marks a notable vegetation shift with the expansion and densification of *Picea mariana* (higher percentage and influx; Figure 3; Supplemental Material S2). It is likely that severe and larger fires promoted the fire-prone *Picea mariana*, as vegetation and soil burning creates suitable conditions for the establishment and regeneration of *Picea mariana* seedlings (Black and Bliss 1980; Viereck 1983). Fire occurrences were particularly low between ca. 4800 and 3600 cal yr BP, but the abundance of the highly flammable *Picea mariana* coincided with particularly dry climatic conditions between 4800 and 4200 cal yr BP (Magnan and Garneau 2014), possibly due

to larger fires during this period (Figure 6). Wet climatic conditions between 4200 and 2600 cal yr BP (Magnan and Garneau 2014) possibly favored *Picea mariana*, thus increasing fuel accumulation, landscape flammability, and biomass burning. Biomass burning was particularly high between ca. 3600 cal yr BP and ca. 2700 cal yr BP. This is in line with the results of other studies in the North American boreal forest indicating that biomass burning peaked between 6000 and 1000 cal yr BP (Ali et al. 2012; Kelly et al. 2013; Remy et al. 2017, 2017), perhaps because of warmer and drier spring and summer conditions (Ali et al. 2012; Remy et al. 2017), and also the increase of landscape flammability following the densification and expansion of *Picea mariana* (Hély et al. 2001; Terrier et al. 2013; Blarquez et al. 2015). In addition, fire occurrences displayed centennial to millennial scale patterns. These changes in wildfire regime could be the result of centennial to millennial scale climatic control on fire activity (Gavin et al. 2006), and to some extent, that of vegetation succession (Blarquez et al. 2015) including other bottom-up controls (e.g., topography, waterbodies; Cyr et al. 2007; Courtney-Mustaphi et al. 2013; Portier et al. 2019).

Open spruce-moss balsam fir-birch forest 1800–300 cal yr BP. A slight increase in fire occurrence between 2000 and 1500 cal yr BP (Figure 6) coupled with very dry climatic conditions between 2600 and 950 cal yr BP (Magnan and Garneau 2014) probably limited tree cover, leading to gradual opening of the vegetation cover as suggested by the total influx decrease until ca. 1000 cal yr BP when it started rising again (Supplemental Material S2) with wetter conditions between 950 and 0 cal yr BP (Magnan and Garneau 2014). By contributing to the opening of the forest landscape (Supplemental Material S2; sharp drop in total pollen accumulation rate), the increase in fire occurrence thus facilitated the deposition of *Carya ovata* (Miller) K. Koch. Pollen, a species that is absent from most nearby regional pollen spectra (e.g., Fréchette et al. 2021) or sparse and considered exotic (Remy et al. 2017). It suggests that the opening of the forest was not limited to the lake Mista catchment area. The late-Holocene decline in total pollen influx was also observed to the southwest (e.g., lake Matamek; Fréchette et al. 2021) and northeast (e.g., lake Eagle; Lamb (1980); lake Moraine and lake Hope Simpson (Engstrom and Hansen 1985)) of our study site. Suitable climatic conditions and smaller or less severe fires enabled *Abies balsamea* and *Picea glauca* to recolonize opened sites by seed rain from survivors in unburned areas (Galipeau et al. 1997; Asselin et al. 2001; Bergeron et al. 2004; Cyr et al. 2012).

Spruce-moss forest 300 cal yr BP to present. Starting ca. 300 cal yr BP, vegetation composition was similar to that of the modern black spruce-moss boreal forest. The relative pollen frequencies of the major taxa are similar to modern pollen spectra percentages obtained from surface sediments of nearby lakes (Lamb 1984; Engstrom and Hansen 1985). *Picea mariana* is the dominant tree in modern pollen assemblages throughout eastern Quebec and Labrador (Fréchette et al. 2021). The pollen influx data from lake Mista (Supplemental Material S2) suggest that the spruce-moss forest opened around 2000 cal yr BP, but without shifting into a spruce-lichen woodland, as it subsequently became denser during the last 300 years.

Fire occurrence and biomass burning were low during the last 300 years, consistent with the decreasing trend in fire frequency (Drobyshev et al. 2017) and burn rates (Chavardès et al. 2022) across eastern Québec from the Little Ice Age to the present. The colder and wetter climatic conditions in the study area (Magnan and Garneau 2014) seem to have helped maintain fire occurrence and biomass burning low despite the high abundance of flammable *Picea mariana* (Figure 6).

Drivers of fire and vegetation trajectories

Compared to the HTM period, the cooler climatic conditions that prevailed during the Neoglacial were less conducive to fire events (Figure 6). Notwithstanding the rising and fluctuating trend of fire occurrence, fires remained less frequent than before 4800 cal yr BP, probably because of the Neoglacial cooler climate conditions linked to decreased solar irradiance (Ali et al. 2012). However, despite less suitable climatic conditions to fire activity, the densification and expansion of *Picea mariana* forests overrode the effects of cooler climate conditions, then led to greater biomass burning and/or larger fires (Figure 4).

The transition from the warm HTM to the cooler Neoglacial period around 4000 cal yr BP does not coincide with the long-term changes in fire regime and vegetation dynamics (Figure 6). A marked decrease in fire frequency occurred around 5000 cal yr BP when the climate was still warm, suggesting that fire occurrence was probably not controlled directly by summer temperature. Other climatic variables (e.g., warm springs, intra-seasonal variability in precipitation, fire season length and drought code; Remy et al. 2017; Portier et al. 2019) could have had a direct control on fire occurrence in eastern Québec at the time.

The shift to spruce-moss forests around 4800 cal yr BP occurred nearly a thousand years before the climatic

shift to the Neoglacial period. This is rather fire that came into play, in particular a decrease in fire occurrence and an increase in fire size or severity (higher magnitude fire peaks starting from ca.4800 cal yr BP; Figure 6). Long-term vegetation changes coincided with shifts from frequent small low-severity fires to infrequent, large, high-severity fires. On the other hand, the shift to higher biomass burning coincides with the shift from spruce-moss balsam fir-birch forest to spruce-moss forest. On a millennial timescale, decreasing summer insolation influenced climate, fire occurrence and vegetation changes. The high abundance of *Betula* (likely *Betula papyrifera*; Fréchette et al. 2021), which is less flammable (Sims et al. 1990), and wet climatic conditions mediated the impacts of HTM warming on biomass burning. Subsequently, the high abundance of flammable *Picea mariana* promoted biomass burning during the Neoglacial.

Vegetation changes at lake Mista may also reflect the influence of other ecological factors operating at various spatial and temporal scales such as climate (annual and seasonal temperature and precipitation), types of surface deposits and soils, and disturbances (fires, insect outbreaks, windthrow) (Sims et al. 1990; Saucier et al. 2009; Couillard et al. 2019a).

Conclusion

The changes in chironomids, pollen, and macroscopic charcoal from the sediment core of Lake Mista disclosed 8500 years of postglacial climate-fire-vegetation interactions. The climate was warmer during the HTM (7000–4000 cal yr BP), then shifted to cooler conditions during the Neoglacial period (4000 cal yr BP to present). However, the long-term changes in summer temperature records are probably not the main factor controlling fire and vegetation dynamics in the Lake Mista area. Throughout the postglacial period, summer temperatures never fell below a threshold that could have induce a significant vegetation response. Other climatic and biophysical variables are probably more important and would need to be studied further.

Acknowledgments

The authors would like to thank Christophe Mavon (Chrono-environnement) for his participation in ^{210}Pb dating of sediment-water interface samples, Véronique Poirier (MFFP) for providing us with the bioclimatic subdomain map, Bi-Tchoko Vincent Evrard Kouadio for helping with the coring and data collection. We thank Michelle Garneau and Hydro-Quebec (RDCPJ 514218-17) for facilitating the access to lake Mista and making the fieldwork possible. The Ministère des Forêts, de la Faune et des Parcs collaborated to the planning and realization of the fieldwork. We deeply thank Pierre J.H. Richard for his comments, corrections and suggestions on our manuscript. We also thank Hugo Asselin, the Editor-in-Chief, and two anonymous reviewers who made comments and recommendations that helped us improve the manuscript.

Disclosure statement

No potential conflict of interest was reported by the authors.

Funding

This research was funded by a Natural Sciences and Engineering Research Council (NSERC) strategic grant to YB, SG, OB and AFT and a NSERC Discovery Grant to OB. This research was also funded by a MITACS grant to AFT, the Centre for Forest Research (CFR) and the CNRS-INSU structuring initiative EC2CO ("CHAZAM" project).

ORCID

Augustin Feussom Tcheumeleu http://orcid.org/0009-0001-1033-3103
Laurent Millet http://orcid.org/0000-0003-2050-206X
Damien Rius http://orcid.org/0000-0002-5793-9292
Yves Bergeron http://orcid.org/0000-0003-3707-3687
Pierre Grondin http://orcid.org/0000-0003-4676-5570
Sylvie Gauthier http://orcid.org/0000-0001-6720-0195
Olivier Blarquez http://orcid.org/0000-0002-1508-6607

Data availability statement

Our data will be archived in an external repository (Figshare) with free access upon acceptance of the manuscript.

References

Ali AA, Blarquez O, Girardin MP, Hély C, Tinquaut F, El Guellab A, Valsecchi V, Terrier A, Bremond L, Genries A 2012. Control of the multimillennial wildfire size in boreal North America by spring climatic conditions. Proc Natl Acad Sci U S A. 109(51):20966–20970. doi: 10.1073/pnas.1203467109.

Andersen T, Cranston PS, Epler JH. 2013. Chironomidae of the Holarctic region: keys and diagnoses – part 1: larvae. Insect systematics and evolution supplement 66. Lund (Scania): Entomological Society of Lund.

Appleby PG, Oldfield F 1978. The calculation of lead-210 dates assuming a constant rate of supply of unsupported ^{210}Pb to the sediment. Catena. 5(1):1–8. doi: 10.1016/S0341-8162(78)80002-2.

Asselin H, Fortin M-J, Bergeron Y 2001. Spatial distribution of late-successional coniferous species regeneration following disturbance in southwestern Quebec boreal forest. For Ecol Manage. 140(1):29–37. doi: 10.1016/S0378-1127(00)00273-5.

Bajolle L, Larocque-Tobler I, Gandouin E, Lavoie M, Bergeron Y, Ali AA 2018. Major postglacial summer temperature changes in the central coniferous boreal forest of Quebec (Canada)

inferred using chironomid assemblages. J Quat Sci. 33 (4):409–420. doi: 10.1002/jqs.3022.

Baltzer JL, Day NJ, Walker XJ, Greene D, Mack MC, Alexander HD, Arseneault D, Barnes J, Bergeron Y, Boucher Y, et al. 2021. Increasing fire and the decline of fire adapted black spruce in the boreal forest. Proc Natl Acad Sci. 118(45):e2024872118. doi:10.1073/pnas.2024872118.

Bennett KD 1996. Determination of the number of zones in a biostratigraphical sequence. New Phytol. 132(1):155–170. doi: 10.1111/j.1469-8137.1996.tb04521.x.

Bergeron Y, Chen HYH, Kenkel NC, Leduc AL, Macdonald SE 2014. Boreal mixed-wood stand dynamics: ecological processes underlying multiple pathways. For Chron. 90 (2):202–213. doi: 10.5558/tfc2014-039.

Bergeron Y, Gauthier S, Flannigan M, Kafka V 2004. Fire regimes at the transition between mixed-wood and coniferous boreal forest in northwestern Quebec. Ecology. 85 (7):1916–1932. doi: 10.1890/02-0716.

Birks HJB, Birks HJB 1998. Numerical tools in paleolimnology – Progress, potentialities, and problems. J Paleolimnol. 20 (4):307–332. doi: 10.1023/A:1008038808690.

Birks HJB, Ter Braak CJF, Line JM, Juggins S, Stevenson AC 1990. Diatoms and pH reconstruction. Phil Trans R Soc Lond Series B Biol Sci. 327(1240):263–278.

Blaauw M 2010. Methods and code for "classical" age-modelling of radiocarbon sequences. Quat Geochronol. 5 (5):512–518. doi: 10.1016/j.quageo.2010.01.002.

Black RA, Bliss LC 1980. Reproductive ecology of *Picea mariana* (Mill.) B.S.P., at tree line near Inuvik, Northwest Territories, Canada. Ecol Monogr. 50(3):331–354. doi: 10.2307/2937255.

Blarquez O, Aleman JC 2015. Tree biomass reconstruction shows no lag in postglacial afforestation of eastern Canada. Can J For Res. 46(4):485–498. doi: 10.1139/cjfr-2015-0201.

Blarquez O, Ali AA, Girardin MP, Grondin P, Fréchette B, Bergeron Y, Hély C 2015. Regional paleofire regimes affected by non-uniform climate, vegetation and human drivers. Sci Rep. 5(1):13356. doi: 10.1038/srep13356.

Borcard DF, Gillet F, Legendre P. 2011. Numerical Ecology with R. New York (NY): Springer.

Bouchard M, Pothier D, Gauthier S 2008. Fire return intervals and tree species succession in the North Shore region of eastern Quebec. Can J For Res. 38(6):1621–1633. doi: 10.1139/X07-201.

Brodersen KP, Quinlan R 2006. Midges as paleoindicators of lake productivity, eutrophication and hypolimnetic oxygen. Quat Sci Rev. 25(15):1995–2012. doi: 10.1016/j.quascirev.2005.03.020.

Brooks SJ, Birks HJB 2001. Chironomid-inferred air temperatures from Lateglacial and Holocene sites in north west Europe: progress and problems. Quat Sci Rev. 20 (16):1723–1741. doi: 10.1016/S0277-3791(01)00038-5.

Brooks SJ, Langdon PG, Heiri O. 2007. The identification and use of palaearctic Chironomidae larvae in palaeoecology. London (UK): Quaternary Research Association.

Brossier B, Oris F, Finsinger W, Asselin H, Bergeron Y, Ali AA 2014. Using tree-ring records to calibrate peak detection in fire reconstructions based on sedimentary charcoal records. Holocene. 24(6):635–645. doi: 10.1177/0959683614526902.

Chavardès RD, Danneyrolles V, Portier J, Girardin MP, Gaboriau DM, Gauthier S, Drobyshev I, Cyr D, Wallenius T, Bergeron Y 2022. Converging and diverging burn rates in North American boreal forests from the little ice age to the present. Int J Wildland Fire. 31(12):1184–1193. doi: 10.1071/WF22090.

Couillard PL, Bouchard M, Laflamme J, Hébert F 2022. Zonage des régimes de feux du Québec méridional. Mémoire de recherche forestière no 189. Québec (QC) : Ministère des Forêts, de la Faune et des Parcs, Direction de la recherche forestière.

Couillard PL, Payette S, Lavoie M, Frégeau M 2018. Macrocharcoal-based chronosequences reveal shifting dominance of conifer boreal forests under changing fire regime. Ecosystems. 21(6):1183–1195. doi: 10.1007/s10021-017-0211-3.

Couillard PL, Payette S, Lavoie M, Frégeau M. 2021. Precarious resilience of the boreal forest of eastern North America during the holocene. For Ecol Manage. 485:118954. doi: 10.1016/j.foreco.2021.118954.

Couillard PL, Payette S, Lavoie M, Laflamme J 2019a. La forêt boréale du Québec : influence du gradient longitudinal. Nat Can. 143(2):18–32. doi: 10.7202/1060052ar.

Couillard PL, Tremblay J, Lavoie M, Payette S. 2019b. Comparative methods for reconstructing fire histories at the stand scale using charcoal records in peat and mineral soils. For Ecol Manage. 433:376–385. doi: 10.1016/j.foreco.2018.11.015.

Courtney-Mustaphi CJ, Davis EL, Perreault JT, Pisaric MFJ 2015. Spatial variability of recent macroscopic charcoal deposition in a small montane lake and implications for reconstruction of watershed-scale fire regimes. J Paleolimnol. 54(1):71–86. doi: 10.1007/s10933-015-9838-2.

Courtney-Mustaphi CJ, Pisaric MFJ, Williams J 2013. Varying influence of climate and aspect as controls of montane forest fire regimes during the late Holocene, southeastern British Columbia. Can J Biogeogr. 40(10):1983–1996. doi: 10.1111/jbi.12143.

Cyr D, Gauthier S, Bergeron Y 2007. Scale-dependent determinants of heterogeneity in fire frequency in a coniferous boreal forest of eastern Canada. Landscape Ecol. 22 (9):1325–1339. doi: 10.1007/s10980-007-9109-3.

Cyr D, Gauthier S, Bergeron Y, Pillar V 2012. The influence of landscape-level heterogeneity in fire frequency on canopy composition in the boreal forest of eastern Canada. J Veg Sci. 23(1):140–150. doi: 10.1111/j.1654-1103.2011.01338.x.

Dalton AS, Margold M, Stokes CR, Tarasov L, Dyke AS, Adams RS, Allard S, Arends HE, Atkinson N, Attig J, et al. 2020. An updated radiocarbon-based ice margin chronology for the last deglaciation of the north American ice sheet complex. Quat Sci Rev. 234:106223. doi: 10.1016/j.quascirev.2020.106223.

De Grandpré L, Gauthier S, Allain C, Cyr D, Périgon S, Pham AT, Boucher D, Morissette J, Reyes J, Aakala T, et al. 2009. Towards an Ecosystem Approach to managing the boreal forest in the North Shore region: disturbance regime and Natural forest dynamics. In Gauthier S, Vaillancourt MA, Leduc A, De Grandpré L, Kneeshaw D, Morin H, Drapeau P, Bergeron Y. (Eds.), Ecosystem management in the boreal forest. 1st. (pp. 229–255). Québec (QC): Presses de l'Université du Québec.

D'Orangeville L, Houle D, Duchesne L, Phillips RP, Bergeron Y, Kneeshaw D 2018. Beneficial effects of climate warming on

boreal tree growth may be transitory. Nat Comm. 9(1):3213. doi: 10.1038/s41467-018-05705-4.

Drobyshev I, Bergeron Y, Girardin MP, Gauthier S, Ols C, Ojal J 2017. Strong gradients in forest sensitivity to climate change revealed by dynamics of forest fire cycles in the post little ice age era. J Geophys Res Biogeosci. 122(10):2605–2616. doi: 10.1002/2017JG003826.

Eggermont H, Heiri O 2012. The chironomid-temperature relationship: expression in nature and paleoenvironmental implications. Biol Rev. 87(2):430–456. doi: 10.1111/j.1469-185X.2011.00206.x.

Engstrom DR, Hansen BCS 1985. Postglacial vegetation change and soil development in southeastern Labrador as inferred from pollen and chemical stratigraphy. Can J Bot. 63 (3):543–561. doi: 10.1139/b85-070.

Fægri K, Iversen J 1989. Textbook of pollen analysis. 4th ed. Chichester (UK): John Wiley and Sons.

Fortin MC, Medeiros AS, Gajewski K, Barley EM, Larocque-Tobler I, Porinchu DF, Wilson SE 2015. Chironomid-environment relations in northern North America. J Paleolimnol. 54(2–3):223–237. doi: 10.1007/s10933-015-9848-0.

Fréchette B, Richard PJH, Grondin P, Lavoie M, Larouche AC. 2018. Histoire postglaciaire de la végétation et du climat des pessières et des sapinières de l'ouest du Québec. Mémoire de recherche forestière no 179. Québec (QC): Ministère des Forêts, de la Faune et des Parcs, Direction de la recherche forestière.

Fréchette B, Richard PJH, Lavoie M, Grondin P, Larouche AC. 2021. Histoire postglaciaire de la végétation et du climat des pessières et des sapinières de l'est du Québec et du Labrador méridional. Mémoire de recherche forestière no 186. Québec (QC): Ministère des Forêts, de la Faune et des Parcs, Direction de la recherche forestière.

Gajewski K. 2015. Quantitative reconstruction of Holocene temperatures across the Canadian Arctic and Greenland. Glob Planetary Change. 128:14–23. doi: 10.1016/j.gloplacha.2015.02.003.

Galipeau C, Kneeshaw D, Bergeron Y 1997. White spruce and balsam fir colonization of a site in the southeastern boreal forest as observed 68 years after fire. Can J For Res. 27 (2):139–147. doi: 10.1139/x96-148.

Gauthier S, Boucher D, Morissette J, De Grandpré L 2010. Fifty-seven years of composition change in the eastern boreal forest of Canada. J Veg Sci. 21(4):772–785. doi: 10.1111/j.1654-1103.2010.01186.x.

Gauthier S, Leduc A, Harvey B, Bergeron Y, Drapeau P 2001. Les perturbations naturelles et la diversité écosystémique. Nat Can. 125(3):10–17.

Gavin DG, Hu FS, Lertzmen K, Corbett P 2006. Weak climatic control of stand-scale fire history during the late Holocene. Ecology. 87(7):1722–1732. doi: 10.1890/0012-9658(2006)87[1722:WCCOSF]2.0.CO;2.

Grimm EC 1987. CONISS: a FORTRAN 77 program for stratigraphically constrained cluster analysis by the method of incremental sum of squares. Comput Geosci. 13(1):13–35. doi: 10.1016/0098-3004(87)90022-7.

Hansen BCS, Engstrom DR 1985. A comparison of numerical and qualitative methods of separating pollen of black and white spruce. Can J Bot. 63(12):2159–2163. doi: 10.1139/b85-305.

Heiri O, Brooks SJ, Birks HJB, Lotter AF 2011. A 274-lake calibration data-set and inference model for chironomid-based summer air temperature reconstruction in Europe. Quat Sci Rev. 30(23):3445–3456. doi: 10.1016/j.quascirev.2011.09.006.

Heiri O, Lotter AF, Hausmann S, Kienast F 2003. A chironomid-based Holocene summer air temperature reconstruction from the Swiss alps. Holocene. 13 (4):477–484. doi: 10.1191/0959683603hl640ft.

Hély C, Flannigan M, Bergeron Y, McRae D 2001. Role of vegetation and weather on fire behavior in the Canadian mixed wood boreal forest using two fire behavior prediction systems. Can J Forest Res. 31(3):430–441. doi: 10.1139/x00-192.

Hennebelle A, Aleman JC, Ali AA, Bergeron Y, Carcaillet C, Grondin P, Landry J, Blarquez O 2020. The reconstruction of burned area and fire severity using charcoal from boreal lake sediments. Holocene. 30(10):1400–1409. doi: 10.1177/0959683620932979.

Higuera PE, Brubaker LB, Anderson PM, Brown TA, Kennedy AT, Hu FS, Chave J 2008. Frequent fires in ancient shrub tundra: implications of Paleorecords for Arctic environmental change. PLoS ONE. 3(3):e0001744. doi: 10.1371/journal.pone.0001744.

Higuera PE, Brubaker LB, Anderson PM, Hu FS, Brown TA 2009. Vegetation mediated the impacts of postglacial climate change on fire regimes in the south-central Brooks range, Alaska. Ecol Monogr. 79(2):201–219. doi: 10.1890/07-2019.1.

Higuera PE, Gavin DG, Bartlein PJ, Hallett DJ 2010. Peak detection in sediment–charcoal records: impacts of alternative data analysis methods on fire-history interpretations. Int J Wildland Fire. 19(8):996–1014. doi: 10.1071/WF09134.

Higuera PE, Peters ME, Brubaker LB, Gavin DG 2007. Understanding the origin and analysis of sediment-charcoal records with a simulation model. Quat Sci Rev. 26(13):1790–1809. doi: 10.1016/j.quascirev.2007.03.010.

Higuera PE, Sprugel DG, Brubaker LB 2005. Reconstructing fire regimes with charcoal from small-hollow sediments: a calibration with tree-ring records of fire. Holocene. 15 (2):238–251. doi: 10.1191/0959683605hl789rp.

Hill MO 1973. Diversity and evenness: a unifying notation and its consequences. Ecology. 54(2):427–432. doi: 10.2307/1934352.

Juggins S 2014. Rioja: analysis of Quaternary science data, R package version. 0.9-3.

Kelly R, Chipman ML, Higuera PE, Stefanova I, Brubaker LB, Hu FS 2013. Recent burning of boreal forests exceeds fire regime limits of the past 10,000 years. Proc Natl Acad Sci U S A. 110(32):13055–13060. doi: 10.1073/pnas.1305069110.

Kelly RF, Higuera PE, Barrett CM, Hu FS 2011. A signal-to-noise index to quantify the potential for peak detection in sediment–charcoal records. Quat Res. 75(1):11–17. doi: 10.1016/j.yqres.2010.07.011.

King GA 1986. Deglaciation and vegetation history of western Labrador and adjacent Quebec [dissertation]. Minneapolis (Minnesota): University of Minnesota.

Lamb HF 1980. Late-Quaternary vegetation history of southeastern Labrador. Arctic And Alpine Res. 12(2):117–135. doi: 10.2307/1550510.

Lamb HF 1984. Modern pollen spectra from Labrador and their use in reconstructing Holocene vegetational history. J Ecology. 72(1):37–59. doi: 10.2307/2260005.

Larocque I. 2008. Nouvelle fonction de transfert pour reconstruire la température à l'aide des chironomides préservés dans les sédiments lacustres. Rapport de Recherche R1032. Québec (QC): Institut Nationale de le Recherche Scientifique.

Larocque I, Rolland N. 2006. A visual guide to sub-fossil chironomids from Québec to Ellesmere Island. Rapport R-900. Québec (QC): Institut Nationale de la Recherche Scientifique.

Larocque-Tobler I 2010. Reconstructing temperature at Egelsee, Switzerland, using North American and Swedish chironomid transfer functions: potential and pitfalls. J Paleolimnol. 44(1):243–251. doi: 10.1007/s10933-009-9400-1.

Larocque-Tobler I 2014. The polish sub-fossil chironomids. Palaeontol Electron. 17:1–29.

Magnan G, Garneau M 2014. Evaluating long-term regional climate variability in the maritime region of the st. Lawrence North Shore (eastern Canada) using a multi-site comparison of peat-based paleohydrological records. J Quat Sci. 29(3):209–220. doi: 10.1002/jqs.2694.

McAndrews JH, Berti AA, Norris G. 1973. Key to Quaternary pollen and spores of the great lakes region. Toronto (Ontario): Royal Ontario Museum.

Medeiros AS, Chipman M, Francis DR, Hamerlik L, Langdon P, Puleo PJK, Schellinger G, Steigleder R, Walker IR, Woodroffe S, et al. 2022. A continent-scale chironomid training set for reconstructing arctic temperatures. Quat Sci Rev. 294:107728. doi: 10.1016/j.quascirev.2022.107728.

Millet L, Rius D, Galop D, Heiri O, Brooks SJ. 2012. Chironomid-based reconstruction of Lateglacial summer temperatures from the Ech palaeolake record (French western pyrenees). Palaeogeogr Palaeoclimatol Palaeoecol. 315:86–99. doi: 10.1016/j.palaeo.2011.11.014.

Millet L, Vannière B, Verneaux V, Magny M, Disnar JR, Laggoun-Defarge F, Walter-Simonnet AV, Ortu E, Bossuet G, De Beaulieu JL 2007. Response of littoral chironomid communities and organic matter to late glacial lake—level, vegetation and climate changes at Lago dell'Accesa (Tuscany, Italy). J Paleolimnol. 38(4):525–539. doi: 10.1007/s10933-007-9088-z.

Morin H, Laprise D, Simon AA, Amouch S. 2009. Spruce budworm outbreak regimes in eastern North America. In: Gauthier S, Vaillancourt M-A, Leduc A, De Grandpré L, Kneeshaw D, Morin H, Drapeau P Bergeron Y, editors Ecosystem management in the boreal forest. 1st ed. Québec (QC): Presses de l'Université du Québec; pp. 156–182.

Mott RJ 1976. A Holocene pollen profil from Sept-îles area, Québec. Nat Can. 103:457–467.

Oksanen J, Blanchet G, Friendly M, Kindt R, Legendre P, MCGlinn D, Minchin PR, O'Hara B, Simpson GL, Solymos P, et al. 2018. Vegan: community ecology package.

Oris F, Ali AA, Asselin H, Paradis L, Bergeron Y, Finsinger W 2014. Charcoal dispersion and deposition in boreal lakes from 3 years of monitoring: differences between local and regional fires. Geophys Res Lett. 41(19):6743–6752. doi: 10.1002/2014GL060984.

Payette S. (1993). The range limit of boreal tree species in Québec-Labrador: an ecological and palaeoecological interpretation. Rev Palaeobot Palynol, 79(1–2), 7–30. doi: 10.1016/0034-6667(93)90036-T

Payette S, Garneau M, Delwaide A, Schaffhauser A 2013. Forest soil paludification and mid-Holocene retreat of jack pine in easternmost North America: evidence for a climatic shift from fire-prone to peat-prone conditions. Holocene. 23(4):494–503. doi: 10.1177/0959683612463099.

Pham AT, De Grandpré L, Gauthier S, Bergeron Y 2004. Gap dynamics and replacement patterns in gaps of the northeastern boreal of Quebec. Can J For Res. 34(2):353–364. doi: 10.1139/x03-265.

Portier J, Gauthier S, Bergeron Y 2019. Spatial distribution of mean fire size and occurrence in eastern Canada: influence of climate, physical environment and lightning strike density. Int J Wildland Fire. 28(12):927–940. doi: 10.1071/WF18220.

Portier J, Gauthier S, Cyr G, Bergeron Y. 2018. Does time since fire drive live aboveground biomass and stand structure in low fire activity boreal forests?Impacts on their management. J Environ Manag. 225:346–355. doi: 10.1016/j.jenvman.2018.07.100.

Portier J, Gauthier S, Leduc A, Arseneault D, Bergeron Y 2016. Fire regime variability along a latitudinal gradient of continuous to discontinuous coniferous boreal forests in eastern Canada. Forests. 7(10):211. doi: 10.3390/f7100211.

R Core Team. 2016. R: a language and environment for statistical computing. Vienna, Austria: R Foundation for Statistical Computing.

Régnière J, Saint-Amant R, Bechard A, Moutaoufik A. 2017. BioSIM 11 – User's manual. Update of information report LAU-X-137. Québec (QC): Laurentian Forestry Centre.

Reimer PJ, Austin WE, Bard E, Bayliss A, Blackwell PG, Ramsey CB, Butzin M, Cheng H, Edwards RL, Friedrich M, et al. 2020. The IntCal20 northern hemisphere radiocarbon age calibration curve (0–55 cal kBP). Radiocarbon. 62(4):725–757. doi:10.1017/RDC.2020.41.

Remy CC, Hely C, Blarquez O, Magnan G, Bergeron Y, Lavoie M, Ali AA 2017. Different regional climatic drivers of Holocene large wildfires in boreal forests of northeastern America. Environ Res Lett. 12(3):035005. doi: 10.1088/1748-9326/aa5aff.

Remy CC, Lavoie M, Girardin MP, Hély C, Bergeron Y, Grondin P, Oris F, Asselin H, Ali AA 2017. Wildfire size alters long-term vegetation trajectories in boreal forests of eastern North America. J Biogeogr. 44(6):1268–1279. doi: 10.1111/jbi.12921.

Renssen H, Seppä H, Crosta X, Goosse H, Roche DM. 2012. Global characterization of the holocene thermal maximum. Quat Sci Rev. 48:7–19. doi: 10.1016/j.quascirev.2012.05.022.

Richard PJH 1970. Atlas pollinique des arbres et de quelques arbustes indigènes du Québec. Nat Can. 97:1–306.

Richard PJH, Fréchette B, Grondin P, Lavoie M 2020. Histoire postglaciaire de la végétation de la forêt boréale du Québec et du Labrador. Nat Can. 144(1):63–76. doi: 10.7202/1070086ar.

Saucier J-P, Baldwin K, Krestov PV, Jorgenson T 2015. Boreal forests. In: Peh K, Corlett R, and Bergeron Y, editors. Routledge handbook of forest ecology. 1st ed. London (UK): Routledge: pp. 7–29.

Saucier J-P, Robitaille A, Grondin P. 2009. Cadre bioclimatique du Québec. In: Doucet R Côté M, editors Manuel de foresterie. 2nd ed. Québec (QC): Éditions Multimondes; pp. 186–205.

Sauvé A 2016. Reconstitution holocène de la végétation et du climat pour les régions de Baie-Comeau et de Havre-Saint-Pierre, Québec [master's thesis]. Montréal (QC) : Université du Québec à Montréal.

Simpson GL 2007. Analogue methods in palaeoecology: using the analogue package. J Stat Softw. 22(2):1–29. doi: 10.18637/jss.v022.i02.

Sims RA, Kershaw HM, Wickware GM. 1990. The autecology of major tree species in the north central region of Ontario. COFRDA report 3302. Forestry Canada. Sault Ste. Marie (Ontario): Great Lakes Forest Research Centre.

Telford RJ, Birks HJB 2011. A novel method for assessing the statistical significance of quantitative reconstructions inferred from biotic assemblages. Quat Sci Rev. 30 (9):1272–1278. doi: 10.1016/j.quascirev.2011.03.002.

Terrier A, Girardin MP, Périé C, Legendre P, Bergeron Y 2013. Potential changes in forest composition could reduce impacts of climate change on boreal wildfires. Ecol Appl. 23(1):21–35. doi: 10.1890/12-0425.1.

Velle G, Brodersen KP, Birks HJB, Willassen E 2010. Midges as quantitative temperature indicator species: Lessons for palaeoecology. Holocene. 20(6):989–1002. doi: 10.1177/0959683610365933.

Velle G, Brooks SJ, Birks HJB, Willassen E 2005. Chironomids as a tool for inferring Holocene climate: an assessment based on six sites in southern Scandinavia. Quat Sci Rev. 24(12):1429–1462. doi: 10.1016/j.quascirev.2004.10.010.

Viereck LA. 1983. The effects of fire in black spruce ecosystems of Alaska and northern Canada. In: Wein R McLean D, editors The role of fire in northern circumpolar ecosystems. Toronto (Ontario): John Wiley and Sons Ltd; pp. 201–220.

Walker IR 1987. Chironomidae (Diptera) in paleoecology. Quaternary Sci Rev. 6(1):29–40. doi: 10.1016/0277-3791(87)90014-X.

Whitlock C, Anderson RS 2003. Fire history reconstructions based on sediment records from lakes and wetlands. In: Veblen T, Baker W, Montenegro G Swetnam T, editors. Fire and climatic change in temperate ecosystems of the western Americas. Ecological studies. Vol. 160, New York (NY): Springer; pp. 3–31.